File Revision Date :

December 8, 2025

Data Set Description:

PI:	Michaël Sicard
Instrument:	Elastic, backscatter lidar “Li1200”
Site:	OPAR-StPaulMaido, Reunion island (21° S, 55° E, 2158 m a.s.l.)
Measurement Quantities:	Vertical profiles of particle backscatter coefficient at 355 nm (3-45 km)

Contact Information:

Name:	Michaël Sicard
Institute:	LACy, UMR 8105 UR CNRS MF, Université de la Réunion
Adresse :	15, avenue René Cassin – CS 92003, 97744 Saint-Denis, France Cédex 9
Phone:	+262 2 62 52 89 63
Email:	michael.sicard@univ-reunion.fr

Instrument Description:

(See Figures 1 and 2) The emission consists in two Nd: YAG Quanta Ray pro 290 lasers, from Spectra-Physics, emitting electromagnetic pulses at 1064 nm and 30 Hz. The final wavelength emitted is 355 nm, which corresponds to the third harmonic of the initial wavelength. Each pulse delivers 375 mJ in 9 ns. The optical design of this lidar is represented in Figure 1. The two laser beams are recombined through a polarizer cube, then sent to the telescope through a series of mirrors. It should be noted that the lasers and the telescope are not in the same room, hence the use of many mirrors. BE1 and BE2 lenses form an afocal of magnification 1.25, reducing the divergence of the beams and mixing the phases. The goal is to reduce the hot spots, especially on the very fragile optic BE3. Last, the laser beam is channeled through the center of the main telescope and magnified by a factor of 10 thanks to the afocal system BE3 and BE4. The emission and main reception are therefore static coaxial, reducing the parallax effect and the minimum overlap altitude.

The reception is made of two telescopes. The main telescope consists in a primary mirror of 1200 mm diameter (M1200), which gave its name to this instrument. A secondary mirror HM sends the beam to the detection system. The L1 lens allows the beam to converge faster, which explains the 3.6 m value of the focal length. GS1 is a glass plate that sends about 8 % of the beam on the 355 nm Very Low (355VL channel) detector. As this detector is located before the FD2 diaphragm, its field of view is the same as the one of the telescopes, and it receives signal in the very near-range. A density (ND) was placed in front of this detector to avoid saturation. FD2 is a diaphragm, located at the focal plane of the telescope. Its aperture improves the geometrical factor of the telescope for the detectors following it. DM1 is a dichroic filter that reflects 355nm and allows 387nm and 407nm to pass through. GS2 is a glass plate that sends about 8% of the beam on the 355 nm Medium (355M) channel and 92% of the beam on the 355nm Hight (355H) channel. DM3 is a dichroic filter which selects the 387 nm for the Raman N2 channel. As of 2017, a second telescope, with a 200 mm M200 primary mirror and a focal length of 1 m, sends the signal to a second detection box, using an optical fiber. This detection box filters the Rayleigh and Raman signals and channels them respectively to the 355L and 387L detectors.

All the detectors are photomultiplier tubes (PMT) from Hamamatsu, reconditioned by the Licel company (http://licel.com). The 355H, 355M, and 355L detectors are electronically shuttered to prevent saturation. The acquisition cards also come from Licel and operate in photocounting mode. There are no analog channels. Raw files follow a 1-minute integration.

Algorithm Description:

Data processing levels range from Level 0 to Level 2.

- Level 0 products (L0) are uncorrected and uncalibrated raw data files in Licel format at full resolution produced by the instrument.
- Level 1 products (L1) provide cloud-free data cleaned from any instrumental artifact (electronic parasites, synchronization problems, power disrupt, etc.). The cloud mask is currently manual. These corrections are essential for any user to be able to apply their own specific aerosol preprocessing without errors linked to the instrument itself or the weather.
- Level 2 products (L2) provide processed lidar data including: saturation correction, background-sky correction, geometrical form factor correction and gluing between high and low-energy channels (L2a). These products also provide the aerosol optical properties and their corresponding uncertainties (L2b).

Only L2b data are publicly available. Most important is the inversion method used. This dataset has been inverted with the two-component Klett inversion (Klett, 1981; 1985) assuming a constant lidar ratio of 50 sr. More details on Level 1 and 2 production can be found in Gantois et al. (2024).

Expected Precision/Accuracy of Instrument:

The total uncertainty budget is described in Appendix B of Gantois et al. (2024) and summarized in Table 1. Four sources of uncertainty were propagated in quadrature (Sicard et al., 2009; Rocadenbosch et al., 2010): (i) uncertainty due to the Rayleigh calibration value, (ii) uncertainty due to the lidar ratio value with a distinction between LR, top and LR, bottom defining the respective upper and lower error bars, (iii) uncertainty due to the SNR vertical distribution, (iv) and uncertainty due to the SNR value at the calibration altitude.

The uncertainty analyses reveal a strong influence of the LR value in the low-altitude ranges and a strong influence of the SNR in the high-altitude ranges. Uncertainty values relative to the total backscatter coefficient are low. Uncertainty values relative to the aerosol backscatter coefficient are high because of the very low aerosol backscatter coefficient values generally observed above Maïdo observatory.

Instrument history and perspectives:

The OPAR Li1200 lidar delivers aerosol optical products (backscatter coefficients at 355 nm) since April 2013. The preprocessed (L1), processed (L2a) and inverted (L2b) data have been performed in an automated and harmonized manner. Uncertainties have been estimated following state-of-the-art formulations of lidar uncertainty budget. The lidar is operated two nights/week on Monday and Tuesday night from approximately 19 to 01:00 LT. During EarthCARE overpasses, measurements are extended until at least 04:00 LT. OPAR-StPaulMaido aerosol lidars are participating to EarthCARE cal/val exercise in the framework of ESA EVID 05 (ACTRIS-EU) and EVID 15 (ACTRIS-FR) projects. Data of this instruments have been used recently in Baron et al. (2023) and Sicard et al. (2025).

A new lidar called TAMARIN (Temperature Aerosol huMidity lidAr at Reunion IslaNd) is currently under development within the CNRS-INSU funded GON lidar project (2022-2025), aiming at a major upgrade and automation of the OHP and OPAR lidar parks. TAMARIN is

designed to measure unmanned, unattended 7 nights/week the profiles of water vapor and aerosols. Elastic parallel, elastic perpendicular and Raman channels are planned at both 355 and 532 nm. TAMARIN should be included in the ACTRIS European research infrastructure and, as such, all optical products will be delivered by the Single Calculus Chain of ACTRIS. When all aerosol products of TAMARIN are validated, only TAMARIN aerosol products will be sent to both ACTRIS and NDACC database.

Reference Articles:

Baron, A., Chazette, P., Khaykin, S., Payen, G., Marquestaut, N., Bègue, N., and Duflot, V.: Early Evolution of the Stratospheric Aerosol Plume Following the 2022 Hunga Tonga-Hunga Ha'apai Eruption: Lidar Observations From Reunion (21°S, 55°E), Geophys. Res. Lett., 50, e2022GL101751, https://doi.org/10.1029/2022GL101751, 2023.

Gantois, D., Payen, G., Sicard, M., Duflot, V., Bègue, N., Marquestaut, N., Portafaix, T., Godin-Beekmann, S., Hernandez, P., and Golubic, E.: Multiwavelength aerosol lidars at the Maïdo supersite, Réunion Island, France: instrument description, data processing chain, and quality assessment, Earth Syst. Sci. Data, 16, 4137–4159, https://doi.org/10.5194/essd-16-4137-2024, 2024.

Klett, J. D.: Stable analytical inversion solution for processing lidar returns, Appl. Opt., 20, 211, https://doi.org/10.1364/AO.20.000211, 1981.

Klett, J. D.: Lidar inversion with variable backscatter/extinction ratios, Appl. Opt., 24, 1638, https://doi.org/10.1364/AO.24.001638, 1985.

Rocadenbosch, F., Md. Reba, M. N., Sicard, M., and Comerón, A.: Practical analytical backscatter error bars for elastic one-component lidar inversion algorithm, Appl. Opt., 49, 3380, https://doi.org/10.1364/AO.49.003380, 2010.

Sicard, M., Comerón, A., Rocadenbosch, F., Rodríguez, A., and Muñoz, C.: Quasi-analytical determination of noise-induced error limits in lidar retrieval of aerosol backscatter coefficient by the elastic, two-component algorithm, Appl. Opt., 48, 176, https://doi.org/10.1364/AO.48.000176, 2009.

Sicard, M., Baron, A., Ranaivombola, M., Gantois, D., Millet, T., Sellitto, P., Bègue, N., Bencherif, H., Payen, G., Marquestaut, N., and Duflot, V.: Radiative impact of the Hunga stratospheric volcanic plume: role of aerosols and water vapor over Réunion Island (21° S, 55° E), Atmos. Chem. Phys., 25, 367–381, https://doi.org/10.5194/acp-25-367-2025, 2025.

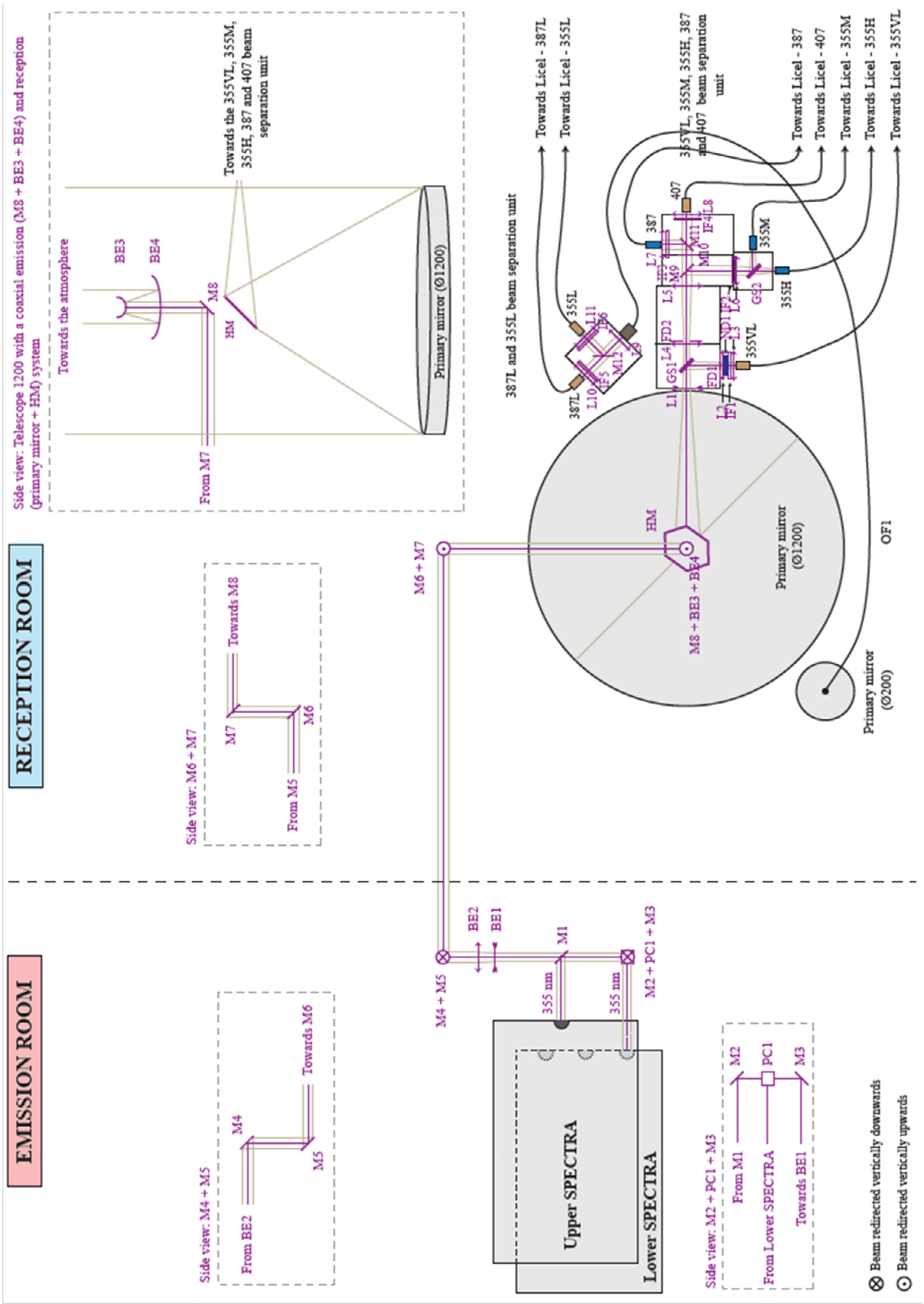

Figure 1: Li1200 optical scheme.

Li1200	ID Optical scheme	Type
Emission	M1, …, M4 and M6, M7	Rmax 355 nm (ø= 1'')
	PC1	0.5'' polarizing cube beamsplitter
	BE1	Lens (f= -200 mm)
	BE2	Lens (f= +250 mm)
	M5	Rmax 355 nm (ø= 40 mm ou 50 mm)
	M8	Rmax 355 nm, dia (ø= 40 mm)
	BE3	Convex mirror (f= +75 mm)
	BE4	Parabolic mirror (f= +900 mm)
Reception	Primary mirror (ø200)	Primary mirror (ø= 0.2 m, f = +1.06 m)
	OF1	Optical fiber (ø= 1.5 mm)
	Primary mirror (ø1200)	Primary mirror (ø= 1.2 m, f= +3.6 m)
	HM	Hexagonal mirror
387L and 355L beam separation unit	L9	Lens (f= +50 mm)
	M12	Longpass filter 376 nm (FF376-Di01)
	IF5	Bandpass filter 386.7-3.0 nm
	L10, L11	Lens (f= +30 mm)
	387L PMT	R9880-113 (BKA0481)
	IF6	Bandpass filter 355-1.3 nm (FF01 356/30-25)
	355L PMT	R9880-113G (BKA0493)
355VL, 355M, 355H, 387 and 407 beam separation unit	L1	Barlow lens (f= -100 mm)
	GS1, GS2	Glass slides 94/6
	FD1	Field iris diaphragm (ø = 5 mm)
	L2, L4	Lens (f= +200 mm)
	ND1	Neutral density filter
	IF1	Bandpass filter 355-1.3nm (LL01-355-25)
	L3, L7	Lens (f= +30 mm)
	355VL PMT	R7400P-03 (HC2228)
	FD2	Field iris diaphragm (ø= 2 mm)
	L5, L6	Lens (f= +100 mm)
	M9	High-pass filter 360 nm (360AELP)
	IF2	Bandpass filter 354.7-1.0 nm
	355M PMT	R7400P-03G (HB9398)
	355H PMT	R7400P-03G (HB9577)
	M10	High-pass filter 370 nm (370AELP)
	M11	High-pass filter 402 nm (402-502-ULTRA)
	IF3	Bandpass filter 386.7-1.0 nm
	387 PMT	R9880-110 (BA2753)
	IF4	?
	L8	?
	407 PMT	?

Figure 2: Specifications of Li1200 optics.

Uncertainty source	Equation
Uncertainty due to the Rayleigh calibration value (u_{altref})	$$u_{altref} = \left\lvert \left(\frac{\beta_j}{\beta_N}\right)^2 \frac{U_N}{U_j} \right\rvert \sigma_{\beta_N}$$
Uncertainty due to the lidar ratio value (u_{LR})	$$u_{LR} = \left\lvert \pm p \frac{2\beta_j^2}{U_j} G_j + p^2 \frac{4\beta_j^3}{U_j^2} {G_j}^2 \right\rvert$$ Where: $G_j = \sum_{i=j}^{N} w_i S_i U_i$
Uncertainty due to the SNR vertical distribution (u_{SNR}).	$$u_{SNR} = \sqrt{\left(\frac{\beta_j}{U_j}\right)^2 \sigma_{U_j}^2 + \left(\frac{2\beta_j}{U_j}\right)^2 \sigma_{GU_j}^2}$$ Where: $\sigma_{GU_j}^2 = \sum_{k=j}^{N} (w_k S_k)^2 {\sigma_{U_k}}^2$
Uncertainty due to the SNR value at the calibration altitude ($u_{SNR,altref}$).	$$u_{SNR,altref} \approx \left\lvert \frac{\beta_j^2}{\beta_N U_j} \right\rvert \sigma_{U_N}$$

Table 1: Total-Backscatter analytical error bars from Klett's backward inversion method (from Rocadenbosch et al., 2010).